Potential impacts of climate warming and increased summer heat stress on the electric grid: a case study for a large power transformer (LPT) in the Northeast United States

Citation: Gao, Xiang, C. Adam Schlosser, and Eric R. Morgan. "Potential Impacts of Climate Warming and Increased Summer Heat Stress on the Electric Grid: a Case Study for a Large Power Transformer (LPT) in the Northeast United States." Climatic Change 147, no. 1–2 (November 20, 2017): 107–118.

As Published: http://dx.doi.org/10.1007/s10584-017-2114-x

Publisher: Springer-Verlag

Persistent URL: http://hdl.handle.net/1721.1/116705

Version: Author's final manuscript: final author's manuscript post peer review, without publisher's formatting or copy editing

Potential Impacts of Climate Warming and Increased Summer Heat Stress on the Electric Grid: A Case Study for a Large Power Transformer (LPT) in the Northeast United States

Xiang Gao[1*], C. Adam Schlosser[1] and Eric Morgan[2]

[*]Corresponding author: xgao304@mit.edu, 617-253-9474

[1]Joint Program on the Science and Policy of Global Change,
Massachusetts Institute of Technology, MA, USA
[2]MIT Lincoln Laboratory, Lexington, MA, USA

Abstract

Large power transformers (LPTs) are critical yet vulnerable components of the power grid. More frequent and intense heat waves or high temperatures can degrade their operational lifetime and increase the risk of premature failure. Without adequate preparedness, a widespread situation could ultimately lead to prolonged grid disruption and incur excessive economic costs. Here we investigate the potential impact of climate warming and corresponding shifts in summertime "hot days" on a selected LPT located in the Northeast United States. We apply an analogue method, which detects the occurrence of hot days based on the salient, associated large-scale atmospheric conditions, to assess the risk of future change in their occurrence. Compared with the more conventional approach that relies on climate model-simulated daily maximum temperature, the analogue method produces model medians of late twentieth-century hot day frequency that are more consistent with observation and have stronger inter-model consensus. Under the climate warming scenarios, multi-model medians of both model daily maximum temperature and analogue method indicate strong decadal increases in hot day frequency by the late 21st century, but analogue method improves model consensus considerably. The decrease of transformer lifetime with temperature increase is further assessed. The improved inter-model consensus of the analogue method is viewed as a promising step toward providing actionable information for a more stable, reliable, and environmentally responsible national grid.

Key words: Electric grid, Heat wave, Climate change, General Circulation Model, Synoptic atmospheric conditions

1. INTRODUCTION

Electricity forms the backbone of nearly every modern society. It is the one sector that most other sectors depend on for their fundamental operations (Pederson et al. 2006). Without electricity, modern society would essentially come to a halt. This is especially true in the United States with its utility grid comprised of thousands of generation units and hundreds of thousands of miles of cables across the entire continent. The intricate electrical network is tasked with maintaining operations nearly 100% of the time, even under extreme weather conditions, shortages of fuel, direct attacks, and human errors. In the United States, prolonged disruptions in electrical service are rare, but cause widespread disorder when they do occur. Events like the Northeast blackout of 2003 (Eto 2004), Hurricane Katrina (Landy 2007), the California energy crisis (Federal Energy Regulatory Commission 2003), and Hurricane Sandy (Hurricane Sandy Rebuilding Task Force 2013) enunciate the problem. During each of these events, electricity was either disconnected or unreliable for extended periods of time, making communications, transportation, sanitation, and public safety vulnerable. Much work and thought has been dedicated to modernizing the grid to make it more resilient to weather related outages, or to terrorist attacks. Indeed, the US government is treating the utility grid as a critical asset and a national security issue (Davis and Clemmer 2014).

Some of the most important yet vulnerable components of the power grid are voltage transformers (Parfomak 2014; U.S. DOE 2012). Transformers are tasked with advantageously boosting or decreasing voltage for transmission so that losses are minimized. One of the failure modes of transformers is over-heating, which degrades the electrical paper insulation and causes catastrophic short circuits. The failure rate is more pronounced as temperature increases, due to more intense chemical reactions that age the insulation. Of particular concern is a subset of the entire network of transformers, namely, “Large Power Transformers” (LPTs) – which are transformers rated at or above 100 MVA (Mega Volt-Amperes). There are thousands of such LPTs across the United States. Moreover, the existing stock of LPTs is old, with 70% or more being 25 years or older out of an expected lifetime of 40 years (U.S. DOE 2015). Added to the burden of overhauling the aging LPT network is the fact that there are very few LPT manufacturers – and many are outside the U.S. and/or overseas. The Department of Homeland Security identified LPTs as a major bottleneck and initiated a program to research and develop temporary recovery transformers (RecX) (The Electric Power Research Institute 2014). While strategies are being developed to modernize the utility grid, the aging fleet is increasingly vulnerable.

Climate change is expected to increase mean temperature and also produce more intense, more frequent, and longer lasting heat waves in many areas of the United States (Meehl and Tebaldi 2004; Melillo et al. 2014). All of these factors can lead to higher consumer demand for electricity, which stresses the already vulnerable fleet of LPTs beyond their design specifications and poses a direct threat to the security of the utility grid. It is therefore important to assess the potential for higher temperatures, more frequent hot days and the subsequent increase in heat stress imposed on LPTs in the coming decades. Currently, studying possible future changes in warm extremes generally employs various indices based on daily maximum and/or minimum temperature simulated with global coupled ocean-atmosphere general circulation models (CGCMs) forced with projected greenhouse gas and aerosol emissions (Meehl and Tebaldi 2004; Sillmann et al. 2013a, b; Russo et al. 2014; Schoetter et al. 2015). These indices largely represent moderately extreme events with re-occurrence times of a year or shorter. Another common approach is

based on the application of an asymptotic extreme value theory for the behavior of extreme events with multi-year to multi-decade re-occurrence times that are of importance to engineering design and planning (Kharin et al. 2007). The results from these studies indicate that climate models capture observed properties of temperature extremes with some fidelity on the global scale (Kharin et al. 2013; Sillmann et al. 2013a), but show limitations at the local scale (Russo et al. 2014; Schoetter et al. 2015). Some efforts are devoted to exploring the physical/dynamical mechanisms causing extreme temperature events and identifying distinctive large-scale atmospheric circulation patterns accompanying them (Grotjahn and Faure 2008; Lau and Nath 2012; Wu et al. 2012). Lau and Nath (2012) found two models employed in their study were capable of reproducing the synoptic features associated with observed heat waves in various North American regions. Grotjahn (2013) demonstrated that daily maximum 2 m temperature from the community Climate System Model version 4 (CCSM4) grid points cannot capture the observed maximum temperature behavior in the California Central Valley, but the circulation index (Grotjahn 2011) constructed with the large-scale upper air circulation features from CCSM4 can provide notable skill in predicting the occurrence of extreme hot surface temperatures.

So far there has been no comprehensive assessment of how skillfully current state-of-the-art climate models simulate the synoptic conditions present during extreme hot temperature events and the role of such conditions in historical and future extreme temperature changes. Gao et al. (2014, 2017) developed an "analogue" approach that creates composites to associate prevailing synoptic atmospheric conditions with heavy precipitation at a local scale and successfully implemented this approach to detect the occurrence of heavy summer and winter precipitation over selected areas of the United States. In particular, when these composites are applied to an ensemble of the Coupled Model Intercomparison Project Phase 5 (CMIP5, Taylor et al. 2012) twentieth-century climate model simulations, more consistent multi-model median of heavy precipitation frequency with observation and a stronger model consensus is achieved compared to using model-simulated precipitation. However, it is not clear whether such an approach will yield similar performance for extreme hot temperature events. Toward the goal of assessing risk of LPTs from future hot days, we prototype this method to detect and predict hot day occurrence at an LPT location in the Northeast corridor of the United States.

First, we describe the procedure for building composites of synoptic-scale daily anomaly circulations that are thermodynamically associated with the "hot" days at a transformer location through a joint analysis of station-based surface daily maximum temperature observations and gridded, daily atmospheric reanalysis data. We then diagnose, calibrate, and evaluate these composites as a predictive analogue for the occurrence of an observed, local "hot day" event. Using CMIP5 simulations, we examine the performance of this analogue approach in reproducing the contemporaneous hot day occurrence against observations as compared to estimates based on climate model-simulated daily maximum air temperature. Projected changes in the hot day occurrence in response to different CMIP5 anthropogenic forcing scenarios are also examined. From these, we assess the economic/cost implications on LPTs from more frequent hot days. Note that the analogue method focuses primarily on the synoptic-scale, thermodynamic processes and conditions linked to the occurrences of locally observed "hot" events. Thus, any local-scale, coupled land-atmosphere processes (i.e. soil moisture, radiative and turbulent heat fluxes, etc.) that would possibly modulate the association of local surface temperature with the large-scale environment are not

explicitly taken into account. As we will show in the evaluation of the analogue's calibration and validation performances (Section 3), these omissions are minimal to the overall interpretations and conclusions that are drawn.

The paper is organized as follows. Section 2 discusses the network analysis used to determine meaningful components within the electric grid and the final selection of transformers based on "betweenness". The climate datasets used in this study is also described. The development, calibration and evaluation of the analogue for hot day occurrence is given in Section 3. In section 4 we discuss the comparative performance of the analogue scheme against simulated daily maximum temperature when applied to CMIP5's late 20th century historical climate as well as future climate under two radiative forcing scenarios, respectively. Section 5 discusses the threat of premature failure in LPTs and potential costs associated with future changes in hot day frequency. Summary and discussions are provided in Section 6.

2. TRANSFORMER SELECTION AND CLIMATE DATASETS

The United States is home to one of the largest connected networks of the electrical system, consisting of over 50,000 substation locations and connected by over 200,000 miles of transmission lines (Eto 2004). We employ graph theory, also known as network analysis, to select the top twenty highest betweenness nodes (transformers) in the Northeastern United States for our analogue method analysis. Further discussion of network analysis is included in the supplementary materials.

The datasets used for this study include the Global Historical Climatology Network-Daily (GHCN-Daily) (Menne et al. 2012), Modern Era Retrospective-analysis for Research and Applications Version 2 (MERRA-2, Bosilovich et al. 2016), and the climate model simulations from the CMIP5 historical experiment (years 1850– 2005) and experiments for the 21st century (years 2006–2100) employing two different radiative forcing scenarios, namely Representative Concentration Pathways (RCP) 4.5 and 8.5 (Taylor et al. 2012). The characteristics of each dataset and relevant data processing are described in the supplementary materials. The GHCN daily maximum temperature from the stations close to the transformers will be used to identify the observed hot days, while the MERRA-2 reanalysis is employed to construct the large-scale composites of atmospheric patterns associated with identified hot days, and to calibrate and evaluate the analogue scheme.

3. CALIBRATION AND EVALUATION OF ANALOGUE METHOD

Currently, there is no universally accepted definition of a "heat wave" event. Several of the more recent definitions are presented in Grotjahn (2011, Table 1), such as consecutive days above a threshold value or percentile and combinations thereof. In this study, the stress from excessive heat on an LPT does not necessarily need to be from a prolonged event (i.e. multiple, consecutive days) and is also more directly associated to exceedance of an absolute temperature (average and/or daily maximum) rather than a more meteorologically-based metric tied to a percentile exceedance. High temperatures affect the peak load capability of an LPT, which can decrease by about 10% at extreme temperatures (Sathaye 2011; Li et al. 2005) and increase the risk of transformer failure (Weekes et al. 2004; Fu et al. 2001), while reducing the operational lifetime (Askari et al. 2009). In this context, we are interested in the deterioration of an LPT associated with a preponderance of days – and anticipated trends in the coming decades - whose temperatures reach or exceed what are incrementally damaging as a result of ambient conditions

and/or load burdens from electricity demands. Given the above considerations, our convention of a "heat wave" is a day in which the daily maximum temperature is at or exceeds 90°F (or ~32°C) at an observation station or model grid, which is further justified by also considering the impact of humidity (as shown in the supplementary materials). In this context, a "heat wave" is viewed more conditionally as a "hot day" – and we will carry this nomenclature hereafter. We performed additional analysis for the high betweenness LPTs we identified to assess availability of nearby GHCN meteorological observations and found an LPT located in southwest Pennsylvania (the red diamond in **Figure 1**). Within a 0.5° radius of the transformer, 7 GHCN stations with daily maximum temperature observations are available. We have selected two of these stations that contained the longest records (20+ years of data) and located at an elevation that is close (within 10s of meters) to that of the LPT. The common hot dates from two these stations are then used for the composite analyses.

Figure 2 shows the composites as standardized anomalies, produced by averaging the MERRA-2 reanalysis atmospheric fields across the 157 observed hot days extracted from the GHCN observations of 1980–2002 for the June-August (JJA) season. The composites indicate that the hot days are associated with large-scale anticyclonic circulation at the mid-levels of the atmosphere (Figure 2 a, b); warm lower tropospheric temperature (at 850 hPa, not shown); and corresponding anomalous positive enthalpy (Fig. 2d) over the transformer area. Also evident are the negative anomalous vorticity (Fig. 2e) over the region and the presence of sinking air to the east and off the coast of the Carolinas that also extends eastward across the Bermuda Islands (Fig. 2c). This large sinking region of air is consistent with the location of the classic "Bermuda High" surface-pressure system, and the associated circulation supports the advection of warm near-surface air from the Gulf of Mexico that is spread across the eastern seaboard of the United States.

All the five composite variables in Figure 2 are used as the basis for the analogue scheme to detect the occurrence of a hot day. We follow the same procedure as described in Gao et al (2017) to develop, calibrate and validate the analogue schemes and briefly review it here. Two metrics, "hotspot" and spatial anomaly correlation coefficient (SACC), are employed to gauge whether the distinct synoptic conditions conducive to hot days identified by the composites (Figure 2) have been replicated on any given day. We perform automatic calibration to determine the cut-off values for SACC and the number of hotspots of all five variables simultaneously. Five performance measures that are commonly used in "confusion matrix" are adopted, including True Positive Rate (TPR), False Positive Rate (FPR), Accuracy (ACC, the ratio of combined true positives (TP) and true negatives (TN) to total population), Precision (PPV, the proportion of correctly identified events to the total identified heavy events), and F1 score (the harmonic mean of PPV and TPR). The optimal cutoff values for SACC and the number of hotspots are achieved by producing the observed number of hot days with the best TPR. The determined detection criteria will be applied to the 2003-2006 MERRA-2 reanalysis as well as the CMIP5 historical and future model-simulated daily meteorological conditions to obtain analogue-based hot days by judging their similarities against the constructed composites. Additional information on detection criteria is included in the supplementary materials.

Table 1 shows performance measures of analogue scheme and MERRA-2 daily maximum temperature in detecting JJA hot days during calibration (1980–2002) and validation (2003– 2006) periods. During the calibration period, the analogue scheme has slightly better performance metrics than the MERRA-2 daily maximum

temperature, with higher TPR, PPV, and F1 score, slightly higher ACC and slightly lower FPR. During the validation period, both analyses strongly overestimate the number of hot days, but the performances of MERRA-2 daily maximum temperature are better than those of analogue scheme. Note that MERRA is not purely model-based, but assimilates a number of observations – primarily states, motions, and transport in the atmosphere throughout both periods. The analogue scheme, however, is evaluated to the data that is independent from the training data used for tuning. Since MERRA is considered to be as close to a global gridded observational dataset as one can find, it is not surprising that it performs well, or outperforms the analogue scheme in some cases. The FPRs and ACC are fairly insensitive measures with minor changes across two periods and two analyses and likely attributed to our unbalanced data set with non-hot days (and thus TN) occupying the large portion. Worthy to note is that the statistics of performance measures during the validation period may not be robust due to relatively short record length.

We also examine the performances of analogue scheme and MERRA-2 daily maximum temperature in depicting the interannual variations of JJA hot day frequency from 1980 to 2002 (calibration) and 2003 to 2006 (validation) and find both analyses to reproduce the observed interannual variations of summer hot day frequency reasonably well. Further discussion is included in the supplementary materials.

4. LATE 20TH CENTURY HOT DAY FREQUENCY AND PROJECTED FUTURE CHANGES

Next we apply the analogue scheme to the CMIP5 late 20th century model simulations. This is achieved by judging the CMIP5 model-simulated daily meteorological conditions of 1980 to 2002 against the constructed composites (e.g. Figure 2) for their similarity in terms of the established "criteria of detection". Any day when the "criteria of detection" are met would be considered as a hot day. **Figure 3a** displays the comparisons of the number of 1980–2002 summer hot days obtained from the CMIP5 model daily maximum temperature and analogue scheme across 20 climate models, from MERRA-2 daily maximum temperature, and from the station observation. Strikingly evident is that the daily maximum temperature-based analyses (the "tasmax") from all the models exhibit a wide degree of estimation and the resulting hot day frequencies demonstrate a wide inter interquartile range (IQR, ≈ 450 days) and inter-model spread (≈ 1035 days). More models tend to underestimate the number of hot days with the multi-model median below the observation. In contrast, the results from the analogue scheme produce more consistent multi-model medians with the observation as well as much reduced IQRs (≈80 days) and inter-model ranges (≈160 days). The central tendency of the analogue scheme slightly overestimates the number of hot days with the observation falling just below the multi-model median. Overall, the analogue scheme improves upon the model daily maximum temperature in the assessment of late 20th century hot day frequency from the perspectives of both accuracy (consistencies of multi-model medians with observation) and precision (inter-model spreads). This demonstrates that state-of-the-art climate models are capable of reproducing the atmospheric synoptic conditions associated with hot days with realistic frequency. Accordingly, the analogue scheme based on resolved large scale circulation features presents collectively better skill in identifying the observed cumulative hot day occurrence compared to estimates from model-simulated daily maximum surface-air temperature.

Figure 3b displays the changes in hot day frequency estimated from an ensemble of CMIP5 model daily

maximum temperature and the analogue scheme under RCP8.5 and 4.5 scenarios. The change is analyzed between the 23-year period of 2070 to 2092 and 2010 to 2032 and expressed as number of days per year. Under the RCP8.5 scenario, the multi-model medians of both analyses indicate pronounced increases in hot day frequency, with medians of both analyses showing about 23 more days/year by the end of the century; this change is nearly quadruple the average number of events (~6) seen every summer through the historical period (1980-2006, see Table 1). All the models from both analyses consistently show the increases in frequency. Inter-model disagreements in the magnitude of change remain larger for model daily maximum temperature than for the analogue result, ranging from increases of 3~48 and 9~37 days per year, respectively. The analogue scheme, however, provides a much reduced IQR (≈7 days), about one-third as much as that of model daily maximum temperature (≈20 days). As expected, the increases in the hot day frequency from both analyses are less pronounced under the lower emission scenario RCP4.5, with multi-model medians showing 8.4 more days/year for daily maximum temperature and 7.2 more days/year for the analogue scheme. However, this median result implies that even under a strong mitigation scenario the number of hot days during JJA will be double that from the historical (1980-2006) period. The mitigation tends to shift not only the multi-model medians but also the entire distributions toward the smaller increases in hot day frequency. Nevertheless, all the models from both analyses show consistency in the sign of change (increase). The inter-model consensuses are largely reduced due to the smaller radiative forcing, ranging from increase of 0.1–22 and 1.6–12 days per year for daily maximum temperature and analogue scheme, respectively. Likewise, the IQR of the analogue result (≈3 days) is about one third as much as that of model daily maximum temperature (≈11 days). Overall, the analogue scheme improves upon model daily maximum temperature by producing a much stronger model consensus in both emission scenarios.

5. ECONOMIC IMPACTS

Failure of a transformer can lead to widespread outages for prolonged periods of time, incurring economic costs in terms of lost wages and productivity (Sullivan et al. 2015). Moreover, the manufacture and delivery of LPTs is a complicated process involving several industries and complex logistics and lead times on LPT replacement can be in the range of years. LPTs are vulnerable to overheating and must be monitored closely to maintain proper operating temperatures. The cooling systems of LPTs are designed such that a threshold temperature of about 90°C – the temperature at which the insulating paper begins degradation (Godina et al. 2015) – is rarely or ever exceeded. The transformer rating (in kVA) is based on a 24-hour average temperature of 30°C (IEEE 2012), and any temperature above this value decreases the KVA rating by about 1% per degree C. The expected lifetime of a transformer is related to the operating temperature which ages the insulating paper between the windings (as shown in the supplementary materials). Using thermal models that describe the top-oil temperature in the transformer as a function of ambient temperature, we can then determine how much oil temperature rise would be expected if the climate is warmed by several degrees (as shown in the supplementary materials). Combining the information above, we find that for a background 1˚C rise in temperature, the lifetime of the transformer decreases by 4 years – or a 10% reduction. Therefore, when considering the RCP4.5 and RCP8.5 end-of-century mean global warming projections over the LPT area of ~2˚C and 4˚C respectively (IPCC 2013 – see e.g. Figure SPM.7), we can extrapolate that the

mean impact on expected transformer lifetime would culminate (by the end of the century) to a range of 20-40%. However, as our hot day assessment has shown, the threat from the occurrence of extreme heat events could double and has the potential to go up by a factor of five (under no mitigation) by the end of the century. To consider more explicitly how more frequent hot days could decrease the expected lifetime and incur additional costs, more advanced models for transformer aging based on the hottest-oil temperature rather than the top oil temperature can be used as a guide (as shown in the supplementary materials).

The economic impact of hot days on LPTs can be given by loss of equipment, as well as the cost of losing service to a large area of electrical customers. For the capital costs of LPTs, the prices are given in (U.S. DOE 2012) as $7,500,000 for a 750 MVA 765–138kV three phase transformer, close to what was listed in Pletka et al. (2014). Moreover, Lawrence Berkeley National Laboratory gives the average per event 8-hour interruption cost for residential customers, small commercial and industrial customers, and medium and large commercial and industrial customers as $17.20, $4,690 and $84,083, respectively (Sullivan et al. 2015). The cost of simply repairing or replacing the transformer goes far beyond the substation walls, and has vast impacts throughout the surrounding area. Critical facilities such as hospitals, places of refuge and emergency services could also be affected, further incurring both economic and potentially human costs.

6. SUMMARY AND DISCUSSION

In this study, we focus on how human-induced changes in climate affect hot days that could then damage the LPTs that are critical to the functioning of the electric power grid in the Northeast corridor of the United States. Methods that assess hot days based on model simulated daily-maximum air temperature pose a challenge for assessing the potential threat or risk – as we have found a weak consensus among model simulations. We develop an analogue method for detecting the occurrence of hot days based on the prevailing large-scale atmospheric conditions ("composites") and eschews the use of model-simulated daily maximum temperature. The composites are constructed for the summer season (JJA) of a targeted LPT location through a joint analysis of station-based daily maximum temperature observation and atmospheric reanalysis. The identified synoptic regimes demonstrate that hot days can be predominantly associated with mid-tropospheric anticyclonic circulation, warm lower tropospheric temperature, and negative vorticity – with all features centered over the area of interest (i.e. approximate location of LPT).

We evaluate the constructed composites as a predictive analogue for hot days. The detection diagnostics of the analogue scheme are first calibrated with 23-year (1980-2002) and then validated with 4–year (2003–2006) MERRA-2 reanalysis. The analogue scheme is found to be comparable to MERRA-2 daily maximum temperature in characterizing the number and interannual variations of observed summer hot days during both periods. With regard to the late 20th century (1980–2002) summer hot day frequencies from an ensemble of CMIP5 models, hot day frequencies based on model-simulated daily maximum temperature exhibit a weak consensus with a wide IQR and inter-model spread. In contrast, the results from the analogue scheme based on the calibrated optimal threshold values produce a more consistent multi-model median with the observation and also have substantially reduced IQR and inter- model range. This indicates that the climate models are able to reproduce the large-scale atmospheric

conditions associated with hot days with realistic frequencies.

The multi-model medians of both model-simulated daily maximum temperature and analogue scheme indicate strong decadal increases in hot day frequency by the end of the 21st century (2070-2092) relative to the 2010-2032 period. The increases are more pronounced under the higher emission scenario (RCP8.5). The mitigation with the lower emission (RCP4.5) tends to shift the multi-model central tendency and distributions toward smaller increases, suggesting that the climate policies adopted in the coming decades will affect the occurrence of hot days. Under both scenarios, all the models from both analyses demonstrate consistency in the sign of change (increase). However, the analogue scheme exhibits much stronger model consensus of the trend (i.e. smaller IQRs) than daily maximum temperature trend estimate.

Notably, the analogue method is implemented under the supposition that large-scale atmospheric conditions play a salient role in the occurrence of an extreme event at the local scale. Thus, alterations of small-scale processes and environments associated with climate change that are not captured by the analogue scheme may introduce a bias in our assessment. Nevertheless, our results indicate that the analogue scheme based on "resolved" large-scale atmospheric features provides skillful assessments of the late 20th century hot day frequencies and a stronger consensus of future change and thus show promise as improved and value-added diagnosis against an evaluation that considers model-simulated daily maximum temperature alone.

We showed that there are economic impacts for LPTs operating at elevated ambient temperatures, as well as during hot days. Higher temperatures are known to degrade the insulation inside the LPTs, putting them at risk for catastrophic failure. Moreover, the degradation is cumulative, so more frequent and more intense hot days could rapidly reduce the lifetime of an LPT, making failure more likely. Failures of LPTs have economic impacts in terms of replacement costs and impacts on the service area associated with the LPT. In this pilot study, the analogue method has been demonstrated to provide a stronger model consensus of trends in future hot day frequency for a particular LPT site of interest, and thus holds promise as a salient stride toward more reliable and actionable climate change information. In particular, for the case of assessing risks of premature failure of our nation's aging network of power transformers, they are very time consumptive and costly to replace and number in the 1,000s. Given these considerations, our future analyses will focus on expanding this analogue method for hot day assessments to provide network coverage of the grid; identify critical junctures/clusters in the grid at high risk; and expand technical and econometric analyses to more explicitly account for the degrading effects and costs of extreme, episodic heatwave events on transformers (as well as other components of the grid). We see this effort as a promising step forward to not only evaluate the potential incurred damage and economic loss, but also inform strategies for a more stable, reliable, and environmentally responsible electric grid.

Acknowledgements

This work was funded by MIT Lincoln Lab (DE-FOA-0000768). We acknowledge the modeling groups, the Program for Climate Model Diagnosis and Intercomparison (PCMDI), and the WCRP's Working Group on Coupled Modeling (WGCM) for their roles in making available the WCRP CMIP5 multimodel dataset. We thank the NOAA Climate Prediction Center for the global gridded precipitation observations and the NASA Global Modeling and Assimilation Office for the MERRA Reanalysis data.

9. REFERENCES

Askari MT, Kadir MZAA, Ahmad WFW, Izadi M (2009) Investigate the effect of variations of ambient temperature on HST of transformer. 2009 IEEE Student Conference on Research and Development (SCOReD), UPM Serdang, pp. 363–367.

Bosilovich MG, Lucchesi R, Suarez M (2016) MERRA-2: File Specification. GMAO Office Note No. 9 (Version 1.1), 73 pp.

Davis M, Clemmer S (2014) Power failure: how climate change puts our electricity at risk and what we can do. Union of Concerned Scientists.

Eto JH (2004) Blackout 2003: final report on the August 14, 2003 blackout in the United States and Canada: causes and recommendations. US Department of Energy, Washington, DC.

Federal Energy Regulatory Commission (2003) Final report on price manipulation in Western markets. Docket No. PA02-2-000, US Department of Energy, Washington, DC.

Fu W, McCalley JD, Vittal V (2001) Risk assessment for transformer loading. IEEE Trans Power Syst **16**: 346–353.

Gao X, Schlosser CA, Xie P, Monier E, Entekhabi D (2014) An Analogue Approach to Identify Heavy Precipitation Events: Evaluation and Application to CMIP5 Climate Models in the United States. J Clim 27: 5941–5963

Gao X, Schlosser CA, O'Gorman PA, Monier E, Entekhabi D (2017) Twenty-First-Century Changes in U.S. Regional Heavy Precipitation Frequency Based on Resolved Atmospheric Patterns. J Clim 30: 2501–2521

Godina R, Rodrigues EM, Matias JC, Catala˜o JP (2015) Effect of loads and other key factors on oil-transformer ageing: sustainability benefits and challenges. Energies 8: 12147– 12186.

Grotjahn R (2011) Identifying extreme hottest days from large scale upper air data: a pilot scheme to find California Central Valley summertime maximum surface temperatures. Clim Dyn 37: 587–604.

Grotjahn R (2013) Ability of CCSM4 to simulate California extreme heat conditions from evaluating simulations of the associ- ated large scale upper air pattern. Clim Dyn 41:1187–1197.

Grotjahn R, Faure G (2008) Composite predictor maps of extraordinary weather events in the Sacramento California region. Weather Forecast 23:313–335.

Hurricane Sandy Rebuilding Task Force (2013) Hurricane Sandy rebuilding strategy: stronger communities, a resilient region. U.S. Department of Housing and Urban Development.

IEEE (2012) IEEE standard test procedure for thermal evaluation of insulation systems for liquid-Immersed distribution and power transformers - Redline. IEEE Std C57.100-2011 pp. 1–55.

IPCC (2013) Summary for Policymakers. In: Stocker TF et al (eds) Climate Change 2013: The Physical Science Basis. Cambridge University Press, Cambridge, United Kingdom and New York, NY, USA.

Kharin VV, Zwiers FW, Zhang X, Hegerl GC (2007) Changes in temperature and precipitation extremes in the IPCC ensemble of global coupled model simulations. J Clim 20: 1419–1444.

Kharin VV, Zwiers FW, Zhang X, Wehner M (2013) Changes in temperature and precipitation extremes in the CMIP5 ensemble. Clim Change 119: 345–357.

Landy M (2007) A failure of initiative: the final report of the select bipartisan committee to investigate the preparation for and response to hurricane Katrina. Publius J Federalism 38:152-65.

Lau N-C, Nath MJ (2012) A model study of heat waves over North America: meteorological aspects and projections for the twenty-first century. J Clim 25:4761–4784.

Li X, Mazur RW, Allen DR, Swatek DR (2005) Specifying transformer winter and summer peak-load limits. IEEE Trans Power Del 20: 185–190.

Meehl G, Tebaldi C (2004) More intense, more frequent, and longer lasting heat waves in the 21st century. Science 305:994–997.

Melillo JM, Richmond TC, Yohe GW (2014) Climate change impacts in the United States: Third National Climate Assessment. U.S. Global Change Research Program.

Menne MJ, Durre I, Vose RS, Gleason BE, Houston TG (2012) An overview of the global historical climatology network-daily database. J Atmos Oceanic Technol 29: 897–910.

Parfomak PW (2014) Physical security of the U.S. power grid: high-voltage transformer substations. Congressional Research Service.

Pederson P, Dudenhoeffer D, Hartley S, Permann M (2006) Critical infrastructure interdependency modeling: a survey of US and international research. Idaho National Laboratory pp. 1–20.

Pletka R, Khangura J, Rawlins A, Waldren E, Wilson D (2014) Capital costs for transmission and substations: updated recommendations for WECC transmission expansion planning, Black and Veatch PROJECT NO. 181374.

Russo S et al (2014) Magnitude of extreme heat waves in present climate and their projection in a warming world. J Geophys Res Atmos 119: 12,500–12,512.

Sathaye J et al. (2011) Estimating risk to California energy infrastructure from projected climate change. LBNL-4967E.

Schoetter R, Cattiaux J, Douville H (2015) Changes of western European heat wave characteristics projected by the CMIP5 ensemble. Clim Dyn 45: 1601–1616.

Sillmann J, Kharin VV, Zhang X, Zwiers FW, Bronaugh D (2013a) Climate extremes indices in the CMIP5 multimodel ensemble: Part 1. Model evaluation in the present climate. J Geophys Res Atmos 118: 1716–1733.

Sillmann J, Kharin VV, Zwiers FW, Zhang X, Bronaugh D (2013b) Climate extremes indices in the CMIP5 multimodel ensemble: Part 2. Future climate projections. J Geophys Res Atmos 118: 2473–2493.

Sullivan MJ, Schellenberg J, Blundell M (2015) Updated value of service reliability estimates for electric utility customers in the United States.

Taylor KE, Stouffer RJ, Meehl GA (2012) An overview of CMIP5 and the experiment design. Bull Amer Meteor Soc 93: 485– 498

The Electric Power Research Institute (2014) Considerations for a power transformer emergency spare strategy for the electric utility industry.

US DOE (2012) Large power transformers and the U.S. electric grid. 55 p.

US DOE (2015) Enabling modernization of the electric power system. In: Quadrennial Technology Review. 22 p.

Weekes T, Molinski T, Li X, Swift G (2004) Risk assessment using transformer loss of life data. IEEE Elect Insul Mag **20**: 27–31.

Wu Z, Lin HL, Li J, Jiang Z, Ma T (2012) Heat wave frequency variability over North America: two distinct leading modes. J Geophys Res 117: D02102.

Table 1. Calibration and validation statistics with the use of five atmospheric variables to construct analogue diagnostics for JJA of transformer T2. TPR, FPR, ACC, PPV, and F1 Score represent true positive rate, false positive rate, accuracy, precision, and F1 score, respectively (See text for details). The numbers highlighted in light gray indicate the better performance in analogue than in MERRA-2 daily maximum air temperature. The numbers highlighted in dark gray indicate the total number of observed hot days.

Scheme	TPR	FPR	ACC	PPV	F1 Score	Total Events
1980-2002 (157)						
MERRA-2	0.484	0.042	0.922	0.478	0.481	159
Analogue	0.516	0.039	0.928	0.516	0.516	157
2003-2006 (11)						
MERRA-2	0.909	0.045	0.954	0.385	0.541	26
Analogue	0.636	0.059	0.932	0.250	0.359	28

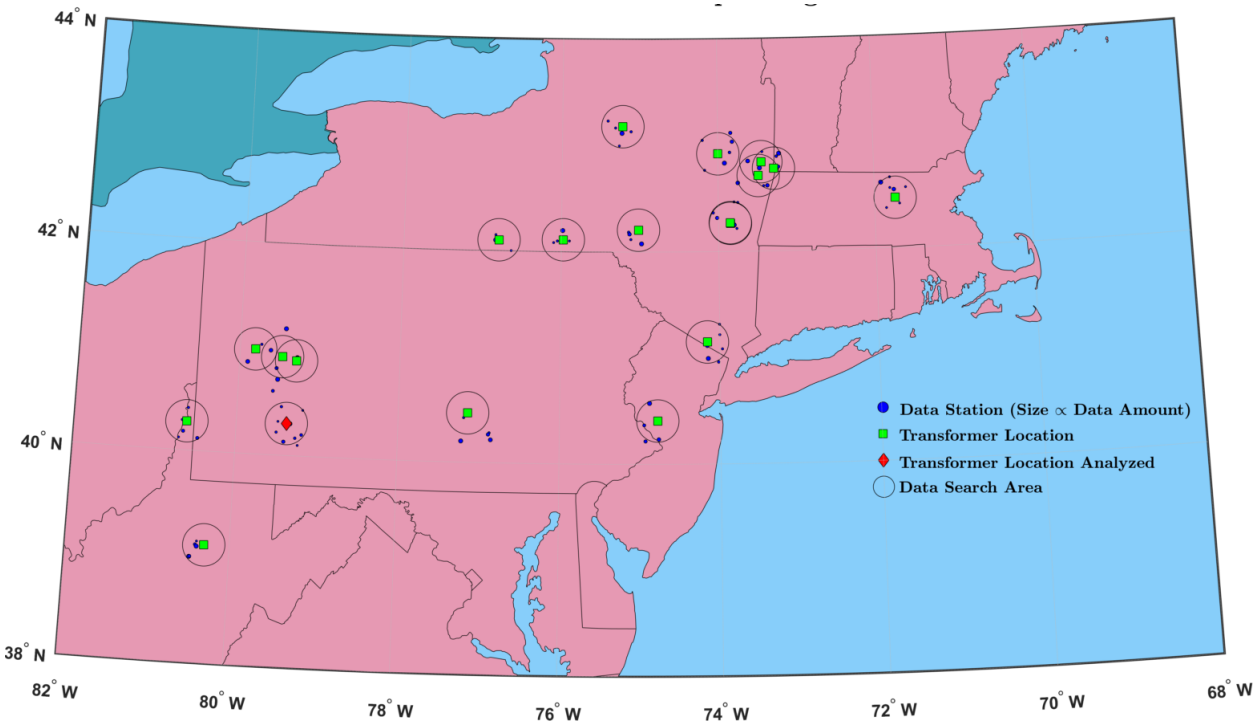

Figure 1. Locations of transformers and weather stations.

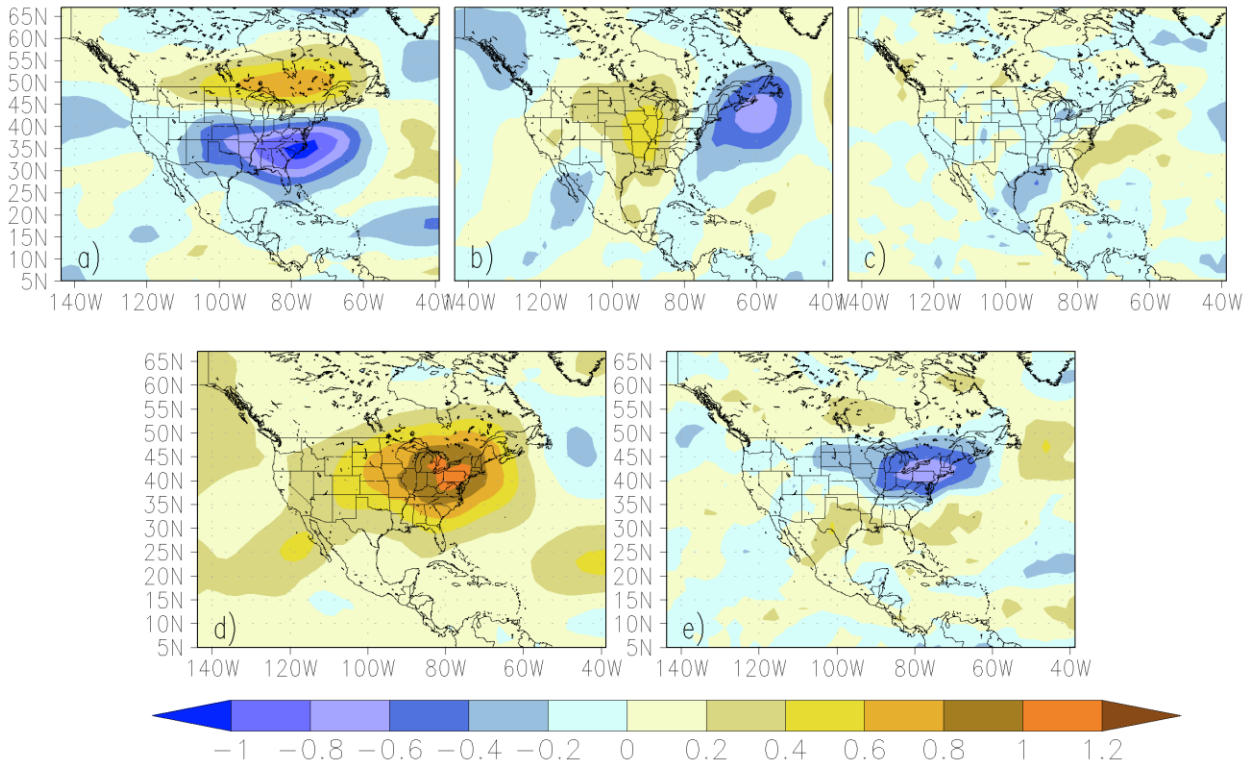

Figure 2. Composite fields as normalized anomalies at 2.5° × 2° for the transformer T2 in JJA: a) 500hPa zonal velocity (u_{500}); b) 500hPa meridional velocity (v_{500}); c) 500hPa vertical pressure velocity (w_{500}); d) vertically integrated enthalpy; and e) 500hPa vorticity (epv_{500}) based on 157 hot days.

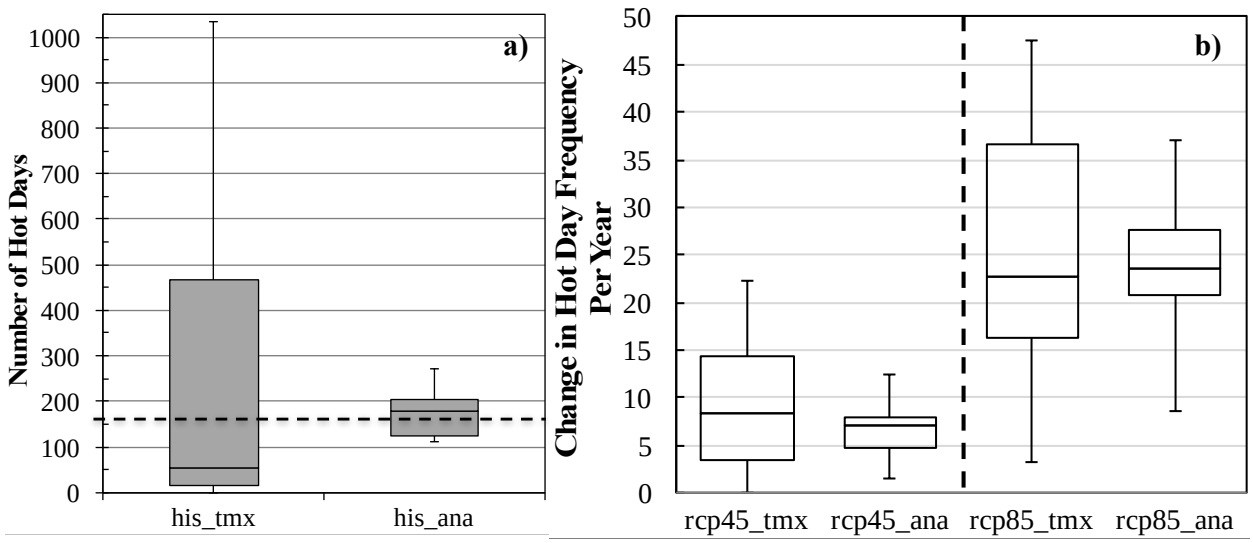

Figure 3. a) Comparisons of the number of summer season (JJA) hot days estimated from CMIP5 model-simulated daily maximum air temperature (his_tmx) and analogue scheme (his_ana) applied to CMIP5 model-simulated atmospheric synoptic conditions during the period of 1980 to 2002. The whisker plot shows the minimum, the lower and upper quartile, median, and the maximum across 20 CMIP5 models. The dashed indicates the number of hot days identified from the GHCN station and MERRA-2 daily maximum air temperature at 2.5º× 2º. The 90ºF is used to extract hot days for all the data sources; b) The changes in hot day frequency between the period of 2070 to 2092 and the period of 2010 to 2032 estimated from an ensemble of CMIP5 model daily maximum air temperature (rcp45_tmx and rcp85_tmx) and synoptic conditions employed by analogue schemes (rcp45_ana and rcp85_ana) under RCP8.5 and RCP4.5 scenarios for JJA of transformer T2.

Article title: Potential Impacts of Climate Warming and Increased Summer Heat Stress on the Electric Grid: A Case Study for a Large Power Transformer (LPT) in the Northeast United States

Journal Name: Climatic Change

Author Names: Xiang Gao, C. Adam Schlosser and Eric Morgan

Corresponding Author:

Xiang Gao, xgao304@mit.edu
Joint Program on the Science and Policy of Global Change,
Massachusetts Institute of Technology, MA, USA

Supplementary File

Contents of the Online Resource:

1. Network analysis for transformer selection:

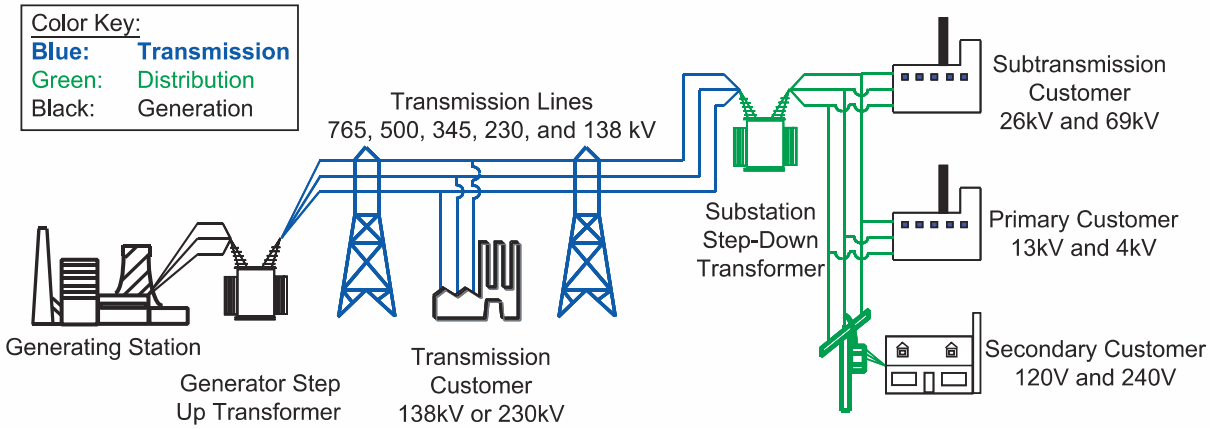

Figure ES1. Generation, Transmission and Distribution Systems in the US (Eto 2004).

Figure ES1 shows the basic layout of the electrical system, beginning with the generation of power and step-up voltage conversion, followed by transmission over large distances, then by step-down voltage conversion. The extreme voltages are employed to minimize power loss, which increases as the square of current. Given the immensity of the electrical grid in the United States, determining key components is a challenging task. Network analysis treats the physical topology of electrical grid as a series of nodes (transformers) and edges (transmission lines) so that basic mathematical analysis can be performed. The mathematics range from simple metrics like the degree of a node (Newman 2010), meaning how many connections it has, to the "betweenness centrality" of a node – a measure of the network's connectivity (Barthelemy 2004). In this work, we chose to use betweenness to select transformers since high betweenness has been shown to be a meaningful parameter for cascading failures in the North American power grid (Kinney et al. 2005; Albert et al. 2004; Bompard et al. 2010). While a discussion of betweenness is beyond the scope of this work, the concept is presented in **Figure ES2**. Here, two networks (Region I and Region II) are connected by a single point, *T*. Thus, all flows between Region I and Region II must utilize T. Severing T will result in two independent regions. Formally, the betweenness of any node *v* measures the fraction of shortest paths flowing through that node (Barthelemy 2004), or:

$$g(v) = \sum_{s \neq v \neq t} \frac{\sigma_{st}(v)}{\sigma_{st}}$$

where σ_{st} is the total number of shortest paths between nodes *s* and *t* and $\sigma_{st}(v)$ is the total number of shortest paths from *s* to *t* via *v*.

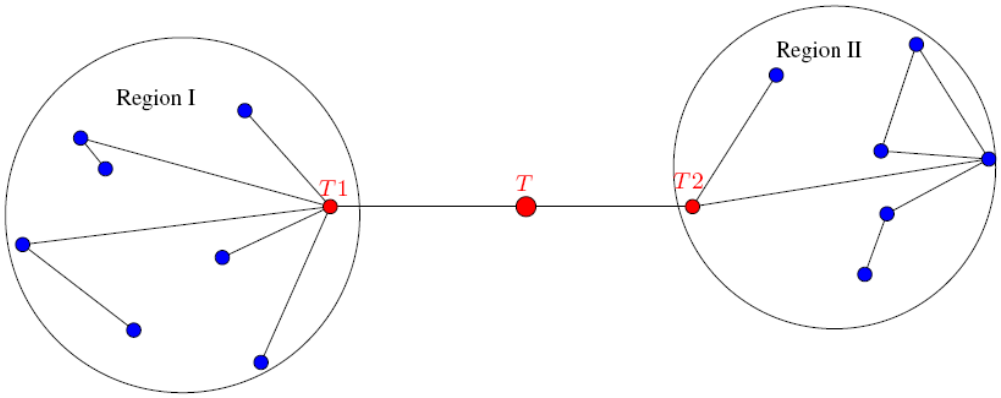

Figure ES2. Node T has high beweenness even though it has few neighbors. Removing T serves the network into two disjoint components.

For simplicity, and to prove the overall concept, we use just the transformers and transmission lines. We omit the generation plants, the distribution lines, and any nodes or edges that are disconnected from the larger system. The final analysis results in 3839 transformers (nodes) connected with 4770 edges (transmission lines). We assume lines to be "undirected", that is power could flow in any direction on the lines. Each transformer is found to, on average, be connected to 2.485 lines. The average path length between two nodes is found to be 18.133, meaning that, on average, more than 18 other nodes are on the path between any two random nodes. We calculate the betweenness centrality for each of the 3839 nodes in the network and create a topological connectivity map, shown in **Figure 3**. The nodes are sized and colored according to their betweenness centrality, with large, green nodes having high betweenness. The lowest betweenness nodes are depicted as small, red dots. We select the top twenty highest betweenness nodes for our analogue method analysis.

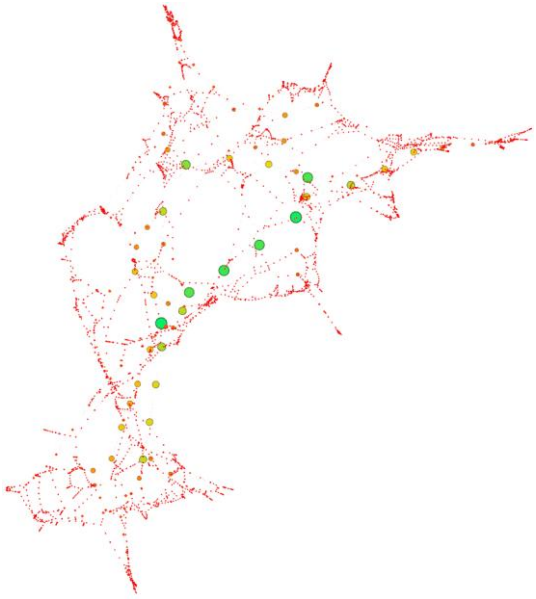

Figure ES3. Northeast US electrical grid network representation using "Betweenness".

2. Datasets

2.1 Observed Daily Maximum Air Temperature

The Global Historical Climatology Network-Daily (GHCN-Daily) is comprised of approximately 27,000 stations globally with daily maximum and minimum temperature. GHCN-Daily is composed of daily weather reports from numerous sources that have been merged and subjected to a common suite of quality assurance (QA) reviews.

2.2 NASA MERRA-2 Reanalysis

In comparison with the MERRA dataset, Modern Era Retrospective-analysis for Research and Applications Version 2 (MERRA-2) represents the advances made in both the Goddard Earth Observing System Model, Version 5 (GEOS-5) and the Global Statistical Interpolation (GSI) assimilation system that enable assimilation of modern hyperspectral radiance and microwave observations, along with GPS-Radio Occultation datasets. MERRA-2 is the first long-term global reanalysis to assimilate space-based observations of aerosols and represent their interactions with other physical processes in the climate system. The MERRA-2 is updated in real time, spanning the period from 1980 to the present. The three-dimensional 3 hourly atmospheric diagnostics on 42 pressure levels are available at a $0.625^{\circ} \times 0.5^{\circ}$ resolution.

2.3 Climate Model Simulations

The CMIP5 historical runs were forced with observed temporal variations of anthropogenic and natural forcings and, for the first time, time-evolving land cover. The future scenarios, called Representative Concentration Pathways (RCPs, Moss et al. 2010), are designed to accommodate a wide range of possibilities in social and economic development consistent with specific radiative forcing paths. The estimated radiative forcing values by year 2100 are 4.5 W/m^2 and 8.5 W/m^2 in the two experiments considered here, namely RCP4.5 and RCP8.5. A total of 20 models provide all the essential meteorological variables for the analogue scheme across the three experiments considered here (**Table 1**). In this study, only one ensemble member from each model is analyzed.

2.4 Data Processing and Analyses

The same set of meteorological variables are assembled or derived from both the MERRA-2 reanalysis and climate model simulations, including 500hPa vector winds (*u500* and *v500*), 500hPa vertical pressure velocity (*w500*), 500hPa vorticity (*epv500*), and vertically integrated enthalpy (*cpt*). The 3-hourly MERRA-2 atmospheric diagnostics are first converted to daily averages. All the daily fields, including the daily maximum air temperature and meteorological fields from MERRA-2 reanalysis and each CMIP5 climate model, are then regridded to a common $2.5^{\circ} \times 2^{\circ}$ resolution via area-weighted averaging. The period with the greatest overlap among the GHCN station data, MERRA-2 reanalysis, and CMIP5 historical experiment is 1 January, 1980 - 31 December, 2002. So at each grid cell, we convert the meteorological fields of each data source to normalized anomalies based on their respective seasonal climatological mean and standard deviation of this 23-yr period. The same seasonal climatological means and standard deviations are also employed to obtain the normalized anomalies for the meteorological fields of MERRA-2 reanalysis from 2003 to 2006 and CMIP5 two RCP experiments from 2006 to 2100. The MERRA-2 reanalysis large scale atmospheric fields from 1980 to 2002 will be used to develop and calibrate the analogue scheme, and from 2003 to 2006 as a provisional validation period.

Table 1. List of the CMIP5 models used for analysis in this study.

Model Name	Country	Resolution	Run	Institution
ACCESS1-0	Australia	192x144L38	1	Commonwealth Scientific and Industrial Research Organization, and Bureau of Meteorology
ACCESS1-3	Australia	192x144L38	1	Commonwealth Scientific and Industrial Research Organization, and Bureau of Meteorology
BCC-CSM1-1	China	128x64L26	1	Beijing Climate Center, China Meteorological Administration
BCC-CSM1-1-m	China	320x160L26	1	Beijing Climate Center, China Meteorological Administration
BNU-ESM	China	128x64L26	1	College of Global Change and Earth System Science, Beijing Normal University
CanESM2	Canada	128x64L35	5	Canadian Centre for Climate Modelling and Analysis
CCSM4	USA	288x192L26	1	National Center for Atmospheric Research
CMCC-CM	Italy	480x240L31	1	Centro Euro-Mediterraneo per | Cambiamenti Climatici
CNRM-CM5	France	256x128L31	1	Centre National de Recherches Meteorologiques
GFDL-CM3	USA	144x90L48	1	Geophysical Fluid Dynamics Laboratory
GFDL-ESM2G	USA	144x90L24	1	Geophysical Fluid Dynamics Laboratory
GFDL-ESM2M	USA	144x90L24	1	Geophysical Fluid Dynamics Laboratory
IPSL-CM5A-LR	France	96x96L39	6	Institut Pierre-Simon Laplace
IPSL-CM5A-MR	France	144x143L39	3	Institut Pierre-Simon Laplace
IPSL-CM5B-LR	France	96x96L39	1	Institut Pierre-Simon Laplace
MIROC5	Japan	256x128L40	5	Atmosphere and Ocean Research Institute, National Institute for Environmental Studies, and Japan Agency for Marine-Earth Science and Technology
MIROC-ESM-CHEM	Japan	128x64L80	1	Japan Agency for Marine-Earth Science and Technology, Atmosphere and Ocean Research Institute, and National Institute for Environmental Studies
CSIRO-MK3.6	Australia	192x96L18	10	Commonwealth Scientific and Industrial Research Organization/Queensland Climate Change Centre of Excellence
MRI-CGCM3	Japan	320x160L48	1	Meteorological Research Institute
NorESM1-M	Norway	144x96L26	3	Norwegian Climate Centre

3. Impact of humidity on daily maximum temperature threshold

For air temperatures exceeding 90°F, its corresponding heat index will exceed 95°F at dew point temperatures equal to or greater than 67°F. Although the GHCN stations do not contain dew point temperatures as part of the archived data, we can use the daily minimum temperature as an approximation for dew point temperature, noting that there are certain conditions when this estimate may be limited (Williams et al. 2015). Upon pooling the minimum temperature data for only the days in which the maximum temperature is equal to or exceeding 90°F, we find that for 20%–30% of those days the dew point is at or above 67°F (**Figure ES4**). In these situations, the transformers would most likely be additionally burdened by electrical demands associated with HVAC cooling.

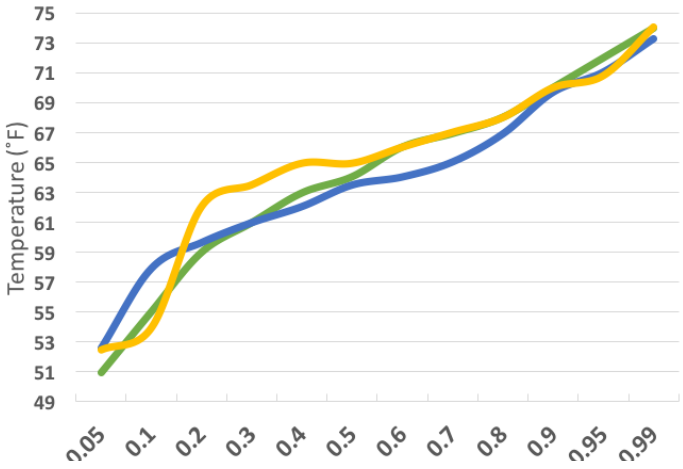

Figure ES4. Cumulative distributions of the estimated (daily) dew point temperature for three of the GHCN stations in proximity to the T2 transformer location. The distributions are constructed by pooling only the days in which the daily maximum temperature is equal to or greater than 90ºF.

4. Analogue detection criteria and analogue evaluation

We follow the similar "criteria of detection" for the analogue scheme in Gao et al. (2014, 2017), but relax them due to the use of more variables in this study by treating two horizontal wind components as two variables corresponding to the trough and ridge of geopotential height and adjusting the cut-off variable number for each metric. The criteria are: 1) At least 4 out of 5 variables have consistent signs with the corresponding composites over the selected "hotspot" grid cells; 2) at least 3 out of 5 variables has SACC larger than the determined thresholds. During the calibration, the daily MERRA-2 atmospheric fields in JJA from 1980 to 2002 is assessed to determine whether the "criteria of detection" described above is met for that day. If so, the day is considered as a hot day.

Analogue scheme and MERRA-2 daily maximum temperature reproduce the observed interannual variations of summer hot day frequency reasonably well with the similar temporal correlations (> 0.85) and root mean square errors (RMSEs, ~ 5days) during both periods. More specifically, we find that they capture more salient multi-year peaks, such as the hot days that occurred in 1983, 1988, 1991, 1995, 1999, 2002 and 2005 as well as valleys in 1990, 1992, 1996, 1998, and 2000. MERRA-2 daily maximum temperature overestimates the observed number of hot days for the summer of 1995, 1999, 2001, 2002, and 2005, but underestimates that for the summer of 1988 and 1994. The analogue scheme strongly underestimates the observed number of hot days for the summer of 1988, but overestimates that for the summer of 1993, 2003, and 2004.

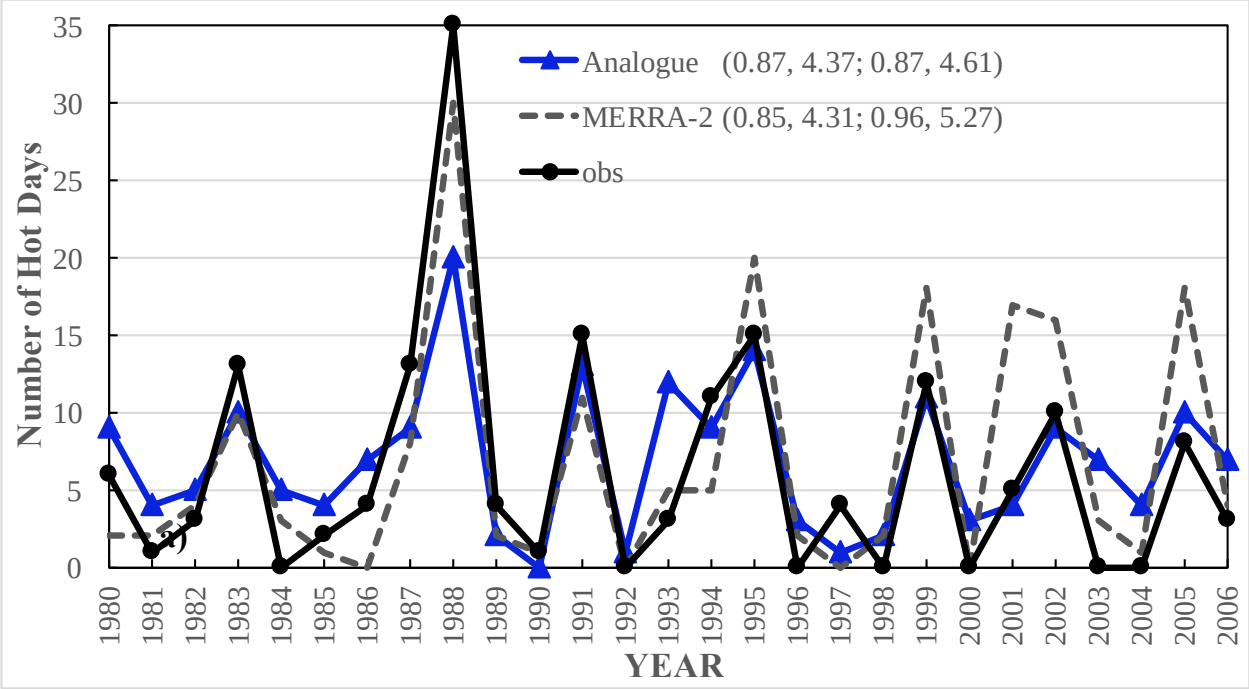

Figure ES5. Comparisons of interannual variations of hot day frequency obtained from analogue scheme, MERRA-2 daily maximum air temperature (MERRA-2), and the observation (obs) for JJA during the calibration (1980–2002) and validation (2003–2006) period. Also shown in the parentheses of figure legend are temporal correlations and RMSE between various schemes and observation during two periods.

5. Economic Impacts

5.1 The expected life of a transformer

Cooling systems for large power transformers (LPTs) are typically oil-based convective heat sinks that circulate oil around the windings of the LPT and transfer the heat to the environment via fans. The systems are not perfect, and often develop "hot spots" within the LPT (Susa and Nordman 2009). These hot spots can damage the insulating paper that protects the windings from short circuits. Such short circuits can severely damage the transformer and lead to sudden, catastrophic failures. The expected life of a transformer is related to the operating temperature which ages the insulating paper between the windings given by Lundgaard et al. (2004):

$$Expected\ Life = \left[\frac{\frac{1}{DP_{End}} - \frac{1}{DP_{Start}}}{A \times 24 \times 365}\right] \exp\left(^{13350}/_{T}\right) \quad (1)$$

where DP_{Start} and DP_{End} are the degree of polymerization of the cellulose at the beginning (≈ 1000) and end of the transformer life (≈ 200), respectively; A is the pre-exponential factor, estimated to be 2E+8, and T is the temperature in Kelvin. Assuming a design life of 40 years (Metwally 2011; U.S. DOE 2012), this corresponds to a temperature of about 82°C and is close to the IEEE standard (IEEE 2012).

5.2 Thermal model for the top-oil temperature in the transformer

Several thermal models that describe the top-oil temperature in the transformer as a function of ambient temperature can be found in Susa et al. (2005) and Tylavsky et al. (2000). A simple thermal model used in this analysis is given by:

$$\theta_{top} = \theta_0 + \theta_{amb} = (\theta_u - \theta_i)(1 - \exp(-t/T_0)) + \theta_i + \theta_{amb} \quad (2)$$

where θ_{top} is the top oil temperature in $^{\circ}$C; θ_o is the initial top oil temperature in $^{\circ}$C; θ_u is the ultimate top rise temperature for a load L in $^{\circ}$C; θ_i is the initial top rise temperature in $^{\circ}$C for time t = 0; and T_O is the time constant at rated power in hours. Equation 2 indicates that a rise in local (ambient) temperature is commensurate with a temperature rise within the transformer.

5.3 Impacts of increased hot days

It is more challenging to explicitly account for the damaging effects of the ambient transformer environment and power demand stress from increased hot days. We draw from previous analyses to present a preliminary synthesis toward a more explicit approach, which is given below. The main standard from IEEE is reviewed here (IEEE 2012). We assume that Equation 2 also holds for the hottest-oil temperature since it is an analogous thermal situation to the analysis presented *vide supra*. The loss of insulation life t_{ei} in an interval t_i, based on the hottest oil temperature, Θ_H, is given for a reference temperature of 383°K as (He et al. 2009; IEEE 1996):

$$t_{ei} = t_i \exp\left(\frac{15000}{383} - \frac{15000}{\Theta_H(t_i)}\right) \quad (3)$$

Then the total loss of insulation for the transformer I_e can be calculated by summing all of the lost insulation life over an interval t_i:

$$I_e = \sum_{i=1}^{n} t_i \exp\left(\frac{15000}{383} - \frac{15000}{\Theta_H(t_i)}\right) \quad (4)$$

The aging failure probability P_a during an interval I_e at reference temperature Θ_O is given by (Billinton and Allan 1992; He et al. 2009)

$$P_a = \frac{F_a(I_e + \Delta t_e|\Theta_O) - F_a(I_e|\Theta_O)}{1 - F_a(I_e|\Theta_O)} \quad (5)$$

where Δt_e is the equivalent operation time. Using Equation 3 along with the definition of conditional probability (Equation 5), a transformer will fail in an interval Δt_e after surviving T years (He et al. 2009):

$$P_a = 1 - exp\left[\left(\frac{I_e}{Cexp\left(\frac{B}{\Theta_O}\right)}\right)^{\beta} - \left(\frac{I_e + \Delta t_e}{Cexp\left(\frac{B}{\Theta_O}\right)}\right)^{\beta}\right] \quad (6)$$

where C and β are the life parameter and shape parameter, respectively.

6. References

Albert R, Albert I, Nakarado GL (2004) Structural vulnerability of the North American power grid. Phys Rev E 69: 025103.

Barthelemy M (2004) Betweenness centrality in large complex networks. Eur Phys J B 38: 163–168.

Billinton R, Allan RN (1992) Reliability Evaluation of Engineering Systems. New York, USA

Bompard E, Wu D, Xue F (2010) The concept of betweenness in the analysis of power grid vulnerability. Complexity in Engineering, pp. 52–54.

Eto JH (2004) Blackout 2003: final report on the August 14, 2003 blackout in the United States and Canada: causes and recommendations. US Department of Energy, Washington, DC.

Gao X, Schlosser CA, Xie P, Monier E, Entekhabi D (2014) An Analogue Approach to Identify Heavy Precipitation Events: Evaluation and Application to CMIP5 Climate Models in the United States. J Clim 27: 5941–5963

Gao X, Schlosser CA, O'Gorman PA, Monier E, Entekhabi D (2017) Twenty-First-Century Changes in U.S. Regional Heavy Precipitation Frequency Based on Resolved Atmospheric Patterns. J Clim 30: 2501–2521

He J, Sun Y, Wang P, Cheng L (2009) A hybrid conditions-dependent outage model of a transformer in reliability evaluation. IEEE Trans Power Del 24: 2025– 2033.

IEEE (1996) IEEE guide for loading mineral-oil-immersed transformers. IEEE Std C57.91-1995.

IEEE (2012) IEEE standard test procedure for thermal evaluation of insulation systems for liquid-Immersed distribution and power transformers - Redline. IEEE Std C57.100-2011 pp. 1–55.

Kinney R, Crucitti P, Albert R, Latora V (2005) Modeling cascading failures in the North American power grid. Eur Phys J B 46: 101–107.

Lundgaard LE, Hansen W, Linhjell D, Painter TJ (2004) Aging of oil-impregnated paper in power transformers. IEEE Trans Power Del **19**: 230–239.

Metwally IA (2011) Failures, Monitoring and new trends of power transformers. IEEE Potentials 30: 36–43.

Moss RH et al. (2010) The next generation of scenarios for climate change research and assessment. Nature 463: 747–756.

Newman M (2010) Networks: An Introduction. Oxford University Press, 720pp

Susa D, Lehtonen M, Nordman H (2005) Dynamic thermal modelling of power transformers. IEEE Trans Power Del 20: 197–204.

Susa D, Nordman H (2009) A simple model for calculating transformer hot-spot temperature. IEEE Trans Power Del 24: 1257–1265.

Tylavsky DJ, He Q, Si J, McCulla GA, Hunt JR (2000) Transformer top-oil temperature modeling and simulation. IEEE Trans Ind Appl 36: 1219–1225.

US DOE (2012) Large power transformers and the U.S. electric grid. 55 p.

Williams MD, Goodrick SL, Grundstein A, Shepherd M (2015) Comparison of dew point temperature estimation methods in Southwestern Georgia. Phys Geogr 36: 255– 267.